Earthquake Engineering, Tenth World Conference © 1992 Balkema, Rotterdam. ISBN 90 5410 060 5

A two dimensional nonstationary optimized accelerogram scaled for magnitude, distance and soil conditions

M. Hammoutene & B.Tiliouine
Civil Engineering Department, Ecole Nationale Polytechnique, Algiers, Algeria

P.Y. Bard
Laboratoire Central des Ponts et Chaussées, Paris & IRIGM, Laboratoire de Géophysique Interne et de Tectonophysique, Observatoire de Grenoble, France

ABSTRACT: An analytical model is presented that allows the simultaneous description of the nonstationary characteristics of the horizontal ground shaking in 2 directions. The parameters of this model are scaled for different soil conditions, epicentral distances and magnitudes from a statistical analysis of 411 worldwide data, leading to 45 different classes. Finally, realistic nonstationary optimized accelerograms are generated for each class.

1 INTRODUCTION

During an earthquake, the characteristics of strong ground motions are influenced by the rupture process of the fault and its size, the travel path of the seismic waves from the source to the receiver, and the local site conditions. These different aspects of the earthquake process affect the nonstationary contents of the recorded accelerograms, in both time and frequency domains.

The aim of this study is to develop an evolutionary spectrum model accounting for the site conditions, epicentral distance and magnitude, and then to generate realistic accelerograms using the scaled models. For this purpose, a statistical investigation is made using a worldwide strong motion data set. The physical spectrum (Mark (1970)) is used as a tool to describe the nonstationary frequency content of the accelerograms. Taking in account the horizontal recorded ground accelerations, we first compute the optimized physical spectra (the maximized and minimized ones), in order to recover the upper and lower bounds of the seismic shaking power, characterizing in this way the two orthogonal components at the site. Then, at each instant, each of the optimized spectra are compared with a gaussian-shaped one, and fitted with three paramters $\omega^o(t)$: the centroïd of the spectrum, $\omega^s(t)$: the dispersion of the spectrum around its centroïd (see Figure 1) and $\alpha(t)$: the ratio factor which made the evolutionary spectrum energy to be equal to the gauss curve area at each instant. The data are divided in 45 different classes taking into account soil conditions S, epicentral distance R and magnitude values M, and the variations of the non-stationary parameters with S, R, and M, are investigated. Making use of the scaled spectrum models coupled with various phase angle distributions, synthetic ground accelerations are constructed for each class.

2 OPTIMIZED SPECTRUM

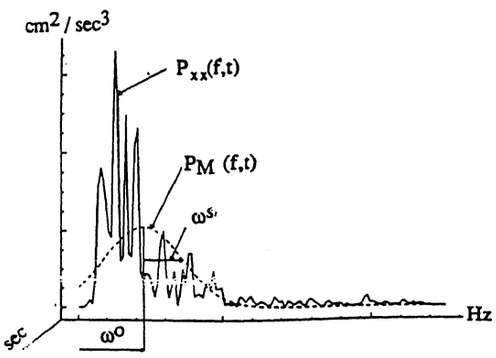

Fig. 1 Gaussian - shaped spectrum P_M (f,t) and its frequency parameters. $P_{xx}(f,t)$ the optimized spectrum

2.1 The physical spectrum

if we considere the acceleration component x(t), its physical spectrum is defined as:

$$P_{xx}(t) = \left| \int_{-\infty}^{\infty} w(t-s)\, x(s)\, e^{-j2\pi fs}\, ds \right|^2 \qquad (1)$$

where f and t represent the frequency and time variables and s a dummy variable. w(t) is a running time window, its functional form is

$$w(t) = 2\,\sigma\sqrt{2\pi}\,\exp\left[-(2\pi\sigma t)^2\right]. \qquad (2)$$

The controlling parameter σ is related to the deviation D (half distance between inflexion points) as

$$D = \frac{\sqrt{2}}{4\pi\sigma} \qquad (3)$$

D is chosen as

$$D = N\,dt\,\sqrt{[2\,Log(2)]} \qquad (4)$$

with N = 128 and dt = 0.02 sec for filtered accelerogram band-width of 0.07-25 Hz (Tiliouine and Azevedo (1984)).

2.2 The optimized physical spectrum

Let us consider the rotation by some angle θ of the two original horizontal accelerograms a(t) and b(t) recorded in the horizontal plane. We define the optimized physical spectra $P_{xx}(f,t)$ and $P_{yy}(f,t)$ and a new set of accelerograms x(t) and y(t) by

$$P_{xx}(f,t) = P_{aa}(f,t)\cos^2(\theta_{cr}) + P_{bb}(f,t)\sin^2(\theta_{cr}) + 2P_{ab}(f,t)\sin(\theta_{cr})\cos(\theta_{cr}) \qquad (5)$$

$$P_{yy}(f,t) = P_{aa}(f,t)\sin^2(\theta_{cr}) + P_{bb}(f,t)\cos^2(\theta_{cr}) - 2P_{ab}(f,t)\sin(\theta_{cr})\cos(\theta_{cr}) \qquad (6)$$

$$\theta_{cr}(f,t) = \frac{1}{2}\,\mathrm{atan}^{-1}\left(\frac{2\,P_{ab}(f,t)}{P_{aa}(f,t) - P_{bb}(f,t)}\right) \qquad (7)$$

where $\theta_{cr}(f,t)$ are the critical directions along which the seismic waves are polarized at each instant and evaluated in order to have $P_{xx}(f,t)$ as the maximized physical spectrum and $P_{yy}(f,t)$ as the minimized one.
$P_{aa}(f,t)$ and $P_{bb}(f,t)$ are the physical spectra of original recorded components a(t) and b(t), $P_{ab}(f,t)$ is the cross-spectrum of a(t) and b(t). It can be noted that $\theta_{cr}(f,t)$ is frequency and time dependent.
The selected model will be scaled to fit $P_{xx}(f,t)$ and $P_{yy}(f,t)$.

3 THE EVOLUTIONARY SPECTRUM MODEL

3.1. expression of the model

The model selected to describe the frequency content is of Gaussian shape, and is expressed as follows:

$$P(\omega,t) = \frac{\alpha(t)}{\sqrt{2\pi}\,\omega^{S}(t)}\exp\left[-\frac{1}{2}\left(\frac{\omega-\omega^{O}(t)}{\omega^{S}(t)}\right)^2\right] \qquad (8)$$

where $\omega^O(t)$, $\omega^S(t)$ are the time varying parameters, defined with the use of the so-called spectral moments (Vanmark (1972)), named respectively the centroïd and the dispersion of the energy centred on the centroïd of the spectrum at the time t. The parameter $\alpha(t)$ is the ratio which ensure the recovery of the original energy under the gaussian curve at each time instant. Indeed, if we consider the evolutionary spectrum $P_{xx}(\omega,t)$ of x(t), then $\alpha(t)$ value is computed as:

$$\alpha(t) = \sqrt{2\pi}\,\omega^{S}(t)\int_{-\infty}^{+\infty} P_{xx}(\omega,t) \Big/ \exp\left[-\frac{1}{2}\left(\frac{\omega-\omega^{O}(t)}{\omega^{S}(t)}\right)^2\right] d\omega \qquad (9)$$

Before carrying out the calculation of the parameters at each time step, a normalization is made so that, the physical spectrum values of each accelerogram were adjusted taking the peak value as unity.

4 REPARTITION AND PROCESSING OF THE DATA

4.1 Selected classes of the data

The method developed previously is applied to a large number (411) of strong motion data recorded in Italy, California, Salvador, Chile, Mexico, Japan and Algeria corresponding to various magnitudes, epicentral distances and site conditions. This data set is divided into 45 different classes, corresponding to 5 magnitude ranges m1 to m5 (m1<4.5, 4.5 ≤ m2 ≤ 5.5, 5.5 ≤ m3≤ 6.5, 6.5 ≤ m4 ≤ 7.5, m5 > 7.5), 3 distance ranges d1 to d3 as shown in Table 1, and 3 site categories s0 to s2(s0 = rock, s1 = stiff soil and s2 = soft soil). Table 2 shows the detail of this selection for each class.

Table 1. Distance ranges

	d1	d2	d2
m 1	< 10	10 - 20	> 20
m 2	< 15	15 - 30	> 30
m 3	< 20	20 - 40	> 40
m 4	< 25	25 - 50	> 50
m 5	< 30	30 - 60	> 60

Table 2. Repartition of the data.

	S0			S1			S2		
	d1	d2	d3	d1	d2	d3	d1	d2	d3
m1	08	07	02	05	05	09	05	07	01
m2	15	05	02	08	07	08	13	02	11
m3	32	06	17	08	11	08	23	19	17
m4	14	05	15	07	29	23	04	18	18
m5	---	---	03	---	02	09	---	---	03
total 1	69	23	39	28	54	57	45	46	50
total 2	131			139			141		

4.2 Data Processing

First, the data have been corrected following the procedure developed by Trifunac and Lee (1973). For a given class, the mean duration of the strong motion is evaluated after making use of the method described in Mc Cann and Shah (1979) at each accelerogram lying in this class. The accelerograms of each class are superimposed in the way of obtaining a coincidence between all the onsets of the strong motion sections. Thus, the first arrivals duration of each accelerogram is considered as the portion located before the beginning of the strong motion one, and the end part of the accelerogram is the one situated after the mean strong motion duration part. The mean duration of both of the latter parts (before and after the strong motion one) is also performed. In this way, the analysed class is represented by an accelerogram wich have as total duration, the sum of the mean durations of every one of the three sections. The procedure described in sections 2 and 3 are then applied to each accelerogram in order to compute its corresponding model parameter values at each instant.

5 STATISTICAL EVALUATION OF THE MODEL PARAMETERS

For each class, a statistical evaluation is performed in order to determine the mean and the 90 percentile values of the parameters ($\omega^0_M(t)$, $\omega^S_M(t)$, $\alpha_M(t)$ and $\omega^0_S(t)$, $\omega^S_S(t)$, $\alpha_S(t)$ respectively) at each time instant. The statistical evaluation for the centroïd is performed in the following way

$$\overset{0}{\omega}_M(t) = \frac{1}{N}\sum_{i=1}^{N} \overset{0}{\omega}_i(t) \qquad (10)$$

$$\overset{0}{\omega}_\sigma(t) = \left[\frac{1}{N-1}\sum_{i=1}^{N}\left(\overset{0}{\omega}_i(t) - \overset{0}{\omega}_M(t)\right)^2\right]^{\frac{1}{2}} \qquad (11)$$

$$\overset{0}{\omega}_S(t) = \overset{0}{\omega}_M(t) + k\,\overset{0}{\omega}_\sigma(t) \qquad (12)$$

$$k = \frac{t_c}{\sqrt{N-1}} \qquad (13)$$

where N is the number of accelerograms of the considered class of (site, distance, magnitude), and t_c is the coefficient related to the student distribution. The same procedure is used in order to compute the values of $\omega^S_M(t)$, $a_M(t)$, $\omega^S_S(t)$ and $\alpha_S(t)$. Two types of modelized physical spectra $P_M(\omega,t)$ and $P_S(\omega,t)$ are obtained with these statistical evaluations:

$$P_M(\omega,t) = \frac{\alpha_M(t)}{\sqrt{2\pi}\,\overset{s}{\omega}_M(t)} \exp\left[-\frac{1}{2}\left(\frac{\omega - \overset{0}{\omega}_M(t)}{\overset{s}{\omega}_M(t)}\right)^2\right] \qquad (14)$$

$$P_S(\omega,t) = \frac{\alpha_S(t)}{\sqrt{2\pi}\,\overset{s}{\omega}_S(t)} \exp\left[-\frac{1}{2}\left(\frac{\omega - \overset{0}{\omega}_S(t)}{\overset{s}{\omega}_S(t)}\right)^2\right] \qquad (15)$$

Figure 2 shows the modelized physical spectra computed with the mean values of the frequency parameters for the s0d1m4 class.

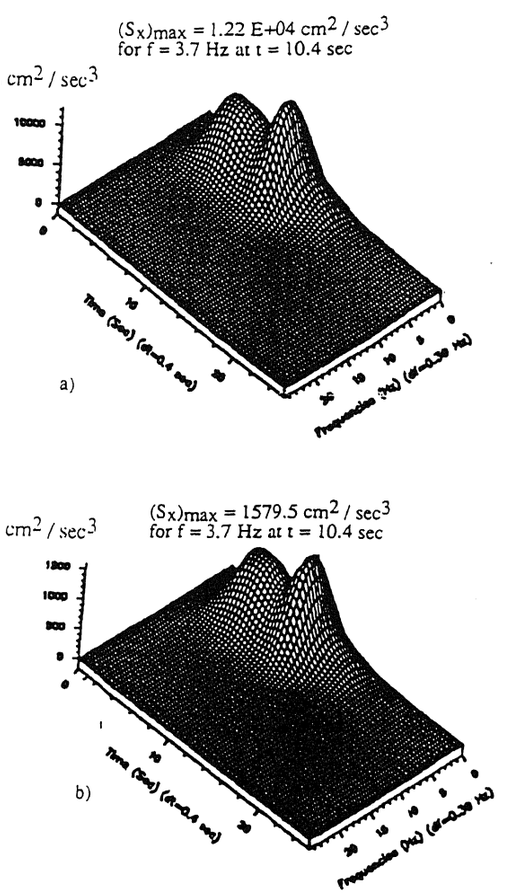

Fig. 2 Evolutionary spectra modelized for s0d1m4 class
a) Maximized evolutionary spectrum (mean value of the frequency parameters)
b) Minimized evolutionary spectrum (mean value of the frequency parameters)

6 RESULTS

6.1 Peak spectrum

The peak spectrum for a given class is defined as the mean of the maximum values of the physical spectra of the corresponding data. Table 3 shows these values for each class. There is a clear trend to a increase with magnitude, this clear trend diminishes for distance d3 for which this increasing character remains only for site s0. On other hand, the peak spectrum value diminishes as the distance increases. This trend is less emphasized for the small magnitudes m1≤ 4.5.

Table 3. Peak spectrum values (10^3 cm^2/sec^3).

	S0			S1			S2		
	d1	d2	d3	d1	d2	d3	d1	d2	d3
m1	0.12	0.05	0.02	0.21	0.03	0.20	0.14	0.10	2.93
m2	0.10	0.48	0.55	2.72	1.04	0.15	2.93	0.09	0.50
m3	3.27	0.69	0.17	4.37	1.11	1.75	2.55	0.72	0.34
m4	12.2	4.36	0.55	10.6	2.55	1.09	8.93	4.74	1.58
m5	---	---	1.13	---	10.5	1.50	---	---	3.58

6.2 Duration of the strong motion parts

The dependency of the duration with the distance is traduced by Table 4. Far stations are characterized by longer durations which are caused by the slow travelling waves trains which arrive late at these stations. This clear trend diminishes for small magnitudes m1 corresponding to very short events. It can be also seen that duration increases with increasing magnitudes. The effect of soils types on duration is traduced by motions on rock sites which have smaller duration than those recorded on soils, this affirmation is less emphasized for near-field stations.

Table 4. Duration of the strong motion parts (sec.).

	S0			S1			S2		
	d1	d2	d3	d1	d2	d3	d1	d2	d3
m1	4.3	4.4	5.1	5.4	3.6	3.4	5.9	5.5	1.6
m2	4.5	4.8	8.5	5.9	8.1	17.6	7.4	10.8	14.4
m3	8.4	11.7	19.7	5.5	12.6	23.0	12.4	17.5	18.1
m4	11.8	17.0	19.8	9.4	16.9	25.3	11.0	16.0	22.8
m5	---	---	48.9	---	33.0	51.5	---	---	41.7

6.3 Frequency parameters variations

In order to study their variations, the values of the central frequency ω^o and the dispersion ω^s are calculated at the instant corresponding to the maximum energy (the higher value of the area under the gauss curve) of the optimized spectrum $P_{M(\omega,t)}$ of each class. The results are reported in Tables 5 and 6.

6.3.1 the centroïd ω^o

The seismologist formulation on the frequency variation is well supported by Table 5 which shows a clear decrease of the central frequency with increasing magnitude. On another hand, the site effect is characterized by higher frequencies on rock sites, this fact is more emphasized for higher magnitudes and far sites.

Table 5. Central frequency variations (Hz).

	S0			S1			S2		
	d1	d2	d3	d1	d2	d3	d1	d2	d3
m1	6.2	6.5	4.6	5.6	6.8	4.8	5.4	7.0	5.5
m2	4.7	7.2	7.8	4.7	5.8	8.9	4.2	6.2	5.7
m3	4.4	5.4	8.7	4.5	5.1	5.4	4.5	3.9	3.9
m4	3.5	3.6	4.8	4.5	2.7	2.7	4.7	3.3	2.9
m5	---	---	2.4	---	3.2	4.5	---	---	1.3

6.3.2 the dispersion ω^s

It can be seen in Table 6 that the variations of the dispersion are not very important for the near field regions (distance d1) but the fluctuations becomes more and more important as the distance increases (distance d2 and d3).

Table 6. Frequency dispersion variations (Hz).

	S0			S1			S2		
	d1	d2	d3	d1	d2	d3	d1	d2	d3
m1	2.6	2.8	2.2	2.9	3.0	2.2	3.1	3.8	2.0
m2	2.4	3.4	2.7	2.8	2.8	3.8	3.1	3.3	3.1
m3	2.8	3.1	4.3	2.5	3.1	3.4	3.1	2.3	2.4
m4	2.8	2.4	2.6	3.0	1.7	1.9	3.0	2.3	1.9
m5	---	---	1.1	---	3.1	3.1	---	---	0.1

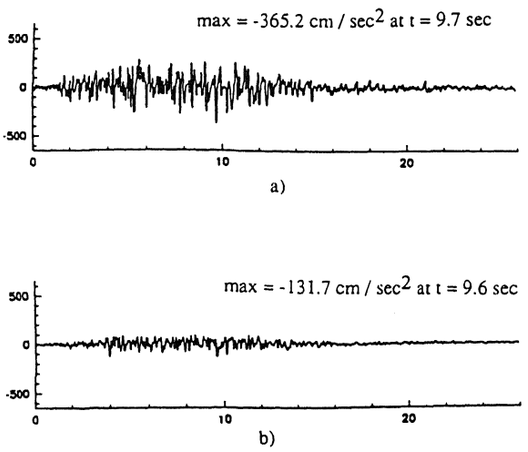

Fig. 3 Simulated accelerograms for s0d1m4 class
a) Maximized simulated accelerogram (mean value of the frequency parameters)
b) Minimized simulated accelerogram (mean value of the frequency parameters)

7 CONCLUSIONS

The statistical investigations developed herein, allow us

to have a simple description of the nonstationary content of the accelerograms via only two frequency parameters ($\omega^0(t)$, $\omega^s(t)$) and one energy parameter ($\alpha(t)$). The parameters have shown to depend on earthquake size, travel path and site conditions. It seems then very important to carry out other investigations which deal with the study of the effect of this nonstationarity on nonlinear structures. That is in fact the following step that we will consider.

REFERENCES

Hammoutene, M., Bard, P. Y. and Tiliouine, B. (1991). A two dimensional model for characterization and simulation of seismic accelerations. European Earthquake Engineering, Volume V - n° 1: 3-9

Mc Cann,M.W.and Shah, H.C. 1979. Determining strong motion duration of earthquakes. Bulletin of Seismological Society of America 69 (4): 1253-1265.

Mark, W.D. 1970. Spectral analysis of the convolution and filtering of nonstationary stochastic process. Journal of Sound and Vibrations, Volume 11: 19-63.

Tiliouine, B. and Azevedo, J. 1984. Stochastic characterization and nonstationary simulation of earthquake accelerograms. 8th World Conference of Earthquake Engineering, San Francisco,Vol. 2: 541-547.

Trifunac,M.D. and Lee, V. 1973. Routine computer processing of strong motion accelerograms. Earthquake Engineering Research Laboratory Report N° 73-03, California Institute of Technology, Pasadena.

Vanmarck,E.H. 1972. Properties of spectral moments with application to random vibrations. Journal of the Engineering Mechanics Division, Proceedings of the American Society of Civil Engineers, Volume 98, N° EM2: 425-446.